Developmental Biology **211,** 109–123 (1999)
Article ID dbio.1999.9297, available online at http://www.idealibrary.com on IDEAL®

Fiber Protein Odf1 and Localizes to Microtubules of Manchette and Axoneme

Xueping Shao,* Heide A. Tarnasky,* Jonathan P. Lee,* Richard Oko,† and Frans A. van der Hoorn*,[1]

**Department of Biochemistry and Molecular Biology, University of Calgary, Calgary, Alberta, Canada T2N 4N1; and †Department of Anatomy and Cell Biology, Queen's University, Kingston, Ontario, Canada K7L 3N6*

Outer dense fibers are structures unique to the sperm tail. No definite function for these fibers has been found, but they may play a role in motility and provide elastic recoil. Their composition had been described before, but only two of the fiber proteins, Odf1 and Odf2, are cloned. We cloned Odf2 by virtue of its functional and specific interaction with Odf1, which, we show, is mediated by a leucine zipper. Further work demonstrated that the 84-kDa Odf2 protein localizes to both the cortex and the medulla of the fibers, whereas the 27-kDa Odf1 protein is present only in the medulla. Here we report the cloning and characterization of a new Odf1-interacting protein, Spag4. Spag4 mRNA is spermatid specific, and the 49-kDa Spag4 protein complexes specifically with Odf1, but not Odf2, mediated by a leucine zipper. It also self-associates. In contrast to Odf1 and Odf2, Spag4 protein localizes to two microtubule-containing spermatid structures. Spag4 is detectable in the transient manchette and it is associated with the axoneme in elongating spermatids and epididymal sperm. Our data suggest a role for Spag4 in protein localization to two major sperm tail structures. © 1999 Academic Press

INTRODUCTION

The flagellum of the mammalian spermatozoon contains characteristic cytoskeletal elements associated with the central axoneme, the most prominent among which are outer dense fibers (ODFs) and the fibrous sheath (FS). Nine ODFs extend throughout the midpiece and principal piece, two of which are replaced by two FS columns in the FS. The FS surrounds the remaining ODFs in the principal region. ODFs differ from one another in terms of their size and cross-sectional profile, and are composed of a central medulla and a thin cortex (Fawcett, 1975). ODFs as well as the FS are resistant to solubilization in ionic detergents (e.g., sodium dodecyl sulfate) because of a high content of disulfide bonds, the extent of which is thought to be regulated by zinc, a constituent of the ODF proteins (Calvin and Bedford, 1971; Calvin and Bleau, 1974; Calvin, 1979), and because the peptides have low solubility (Shao and van der Hoorn, 1996). The investigation of protein components of rat ODFs has revealed multiple polypeptides including several major (32, 27.5, 20, 14.4, 84, and 80 kDa) and minor peptides on the basis of their relative mobility in sodium dodecyl sulfate–polyacrylamide gel electrophoresis (SDS–PAGE) (Calvin, 1979; Olson and Sammons, 1980; Vera *et al.*, 1984; Oko and Clermont, 1988). These polypeptides are found to be phosphorylated at serine residues, with yet unknown roles in sperm motility (Olson and Sammons, 1980; Vera *et al.*, 1984; Oko and Clermont, 1988). The FS is also composed of multiple polypeptides. The components of ODFs and the FS are related in terms of antigenic determinants and size (Oko, 1988). ODFs and the FS also share antigenic determinants with cytoskeletal components in the connecting piece and perinuclear theca in the sperm head (Oko, 1988; Oko and Clermont, 1988). The morphogenesis of ODFs and the FS along the axoneme has been well defined in the rat. ODFs are assembled in a proximal-to-distal direction in step 8 to 19 spermatids, while the FS is assembled in a distal-to-proximal direction in step 2 to 17 spermatids (Irons and Clermont, 1982a, b). The synthesis of

[1] To whom correspondence should be addressed at Department of Biochemistry and Molecular Biology, University of Calgary, 3330 Hospital Drive NW, Calgary, Alberta, Canada T2N 4N1. Fax: (403) 283–8727. E-mail: fvdhoorn@ucalgary.ca.

0012-1606/99 $30.00

ODF and FS polypeptides in the cytoplasm of elongating spermatids, many of which are probably encoded by testis-specific genes, corresponds to the growth of both these cytoskeletal structures along the spermatid flagellum as revealed by immunocytochemical studies using antibodies against the major ODF and FS polypeptides (Oko and Clermont, 1989). The translation of these proteins, which occurs after the condensation of the spermatid nucleus when mRNA synthesis stops, is likely under translational control (Oko and Clermont, 1989).

The study of ODF function in sperm motility is hampered by the uncertain identity and insoluble nature of individual ODF components. Earlier biochemical analysis and structural studies had suggested that ODFs probably function as passive elastic structures and provide elastic recoil for the sperm tail (Fawcett, 1975). It has been demonstrated recently that the ODFs appear to protect sperm against shear forces (Baltz *et al.*, 1990). It is very likely that the function of ODFs and the FS relies on the networks formed by specific protein–protein interactions between individual ODF and FS protein components. However, little is known about the molecular interactions that occur during morphogenesis of ODFs and FS due to the fact that very few genes encoding such proteins have been isolated and characterized. Recently, a small number of proteins that bind FS have been cloned, including the 82-kDa major mouse fibrous sheath protein, which is expressed in spermatids and is related to A-kinase anchoring proteins, glutathione *S*-transferase, hexokinase 1, and glyceraldehyde phosphate dehydrogenase (Carrera *et al.*, 1994; Fulcher *et al.*, 1995; Westhoff and Kamp, 1997; Mori *et al.*, 1998). A gene encoding one of the most abundant ODF proteins, Odf1, was recently cloned and identified by three groups using different methods (Odf1 is also referred to as RT7 and Odf27) (van der Hoorn *et al.*, 1990; Burfeind and Hoyer-Fender, 1991; Morales *et al.*, 1994).

Odf1 is specifically and abundantly expressed in round spermatids (van der Hoorn *et al.*, 1990). The Odf1 promoter has been analyzed by *in vitro* transcription using rat seminiferous tubule-derived nuclear extracts, and it is activated by the spermatid-specific transcription factor CREMτ (van der Hoorn and Tarnasky, 1992; Delmas *et al.*, 1993). Sequence analysis predicted that the Odf1 protein contains an N-terminal amphipathic α helix (van der Hoorn *et al.*, 1990) that resembles the amphipathic leucine zipper found in transcription factors of the basic leucine zipper (bZIP) type (Vinson *et al.*, 1989) as well as in some cytoskeletal proteins (Lewis *et al.*, 1989). The C terminus of Odf1 contains tripeptide repeats of Cys–Gly–Pro (CGP) and variations thereof which are also present in the *Drosophila* Mst87F [previously called mst(3)gl-9] gene product (Schafer, 1986), a member of the Mst(3)CGP gene family (Kuhn *et al.*, 1988, 1991; Schafer *et al.*, 1993). The Mst(3)CGP genes are transcribed exclusively in the male germ line of *Drosophila* and encode satellite fibers in sperm tail that are structural analogs of mammalian ODFs (Kuhn *et al.*, 1988, 1991; Schafer *et al.*, 1993). The Odf1 protein most likely contains an extended rodlike structure, and both the N-terminal leucine zipper motif and the C-terminal CGP repeats are responsible for the weak self-interaction of Odf1 protein (Shao and van der Hoorn, 1996). This suggests that Odf1 protein may interact with itself as well as with other ODF proteins or sperm tail proteins during ODF morphogenesis. Using the N-terminal region of Odf1 as a bait in a yeast two-hybrid screen, we recently identified another major ODF protein, Odf2 (previously called Odf84), which is expressed specifically and abundantly in testis (Shao *et al.*, 1997). The predicted amino acid sequence of Odf2 contains two putative leucine zipper motifs in the C-terminal region, the upstream one of which is specifically involved in the interaction with the leucine zipper domain of Odf1 (Shao *et al.*, 1997). That study also demonstrated that Odf2 localizes to ODFs. In a recent study (Schalles *et al.*, 1998) we show that although Odf1 and Odf2 are both detected in ODF, they show significant differences in sub-ODF localization: Odf2 is present in both the cortex and medulla of ODF. Odf1 is detectable only in the medulla. Both proteins can also be detected in the sperm tail connecting piece.

Here, we report the identification and characterization of a second Odf1-interacting protein, Spag4, which, like Odf1, is exclusively transcribed in round spermatids and translated in elongating spermatids. However, in contrast to Odf1, Spag4 protein appears to be associated with the axonemal and manchette microtubules during sperm tail formation. We also uncovered a second protein interaction domain in Spag4 responsible for self-association, which differs from the Spag4 leucine zipper motif. These observations suggest that Spag4 protein assists during the organization and assembly of ODFs in the elongating spermatids.

MATERIALS AND METHODS

Library Constructions and Screening

The construction of the pGAD/testicular cDNA expression library and λgt11 testicular cDNA expression library was described elsewhere (Shao *et al.*, 1997). The yeast two-hybrid screening procedures including yeast transformation, β-galactosidase activity filter assay, plasmid DNA isolation and preparation, and false-positive elimination were described previously (Shao *et al.*, 1997).

In Vitro Translation and Immunoprecipitation

The insert of pGAD/55-800 was subcloned into pBS-ATG (Shao *et al.*, 1997) as an *Eco*RI–*Sal*I fragment, generating plasmid pBS-ATG-800. *In vitro* translations (or cotranslations) of pBS-ATG-800 and pET/RT7NT [Higgy *et al.*, 1994] were performed using the T7 (RNA polymerase) TNT system (Promega) in the presence of [^{35}S]Cys as described previously (Shao *et al.*, 1997).

Spermatids were obtained by centrifugal elutriation of SD rat spermatogenic cells as described previously (Grootegoed *et al.*, 1977; Delmas *et al.*, 1993). Spermatid mRNA was isolated using the Quick-prep *Micro* mRNA Purification Kit (Pharmacia) as recommended by the manufacturer. *In vitro* translation of spermatid mRNA was performed in a reticulocyte lysate system (Promega)

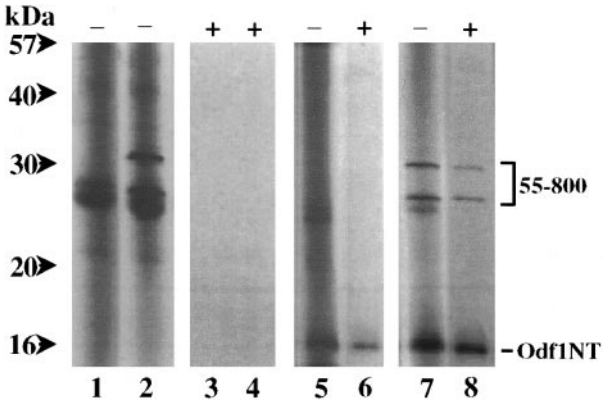

FIG. 1. *In vitro* interaction of Spag4 and Odf1. PBS-ATG/800 and pET/RT7NT clones were *in vitro* translated individually and analyzed by SDS–PAGE directly (lanes 2 and 5, respectively) or after immunoprecipitation with T7·tag antibody (lanes 4 and 6, respectively; addition of antisera indicated by the "+"). Only epitope tagged Odf1NT is recognized by the antibody (lane 6). Control translations contained water (lanes 1 and 3). PBS-ATG/800 and pET/RT7NT clones were next cotranslated *in vitro* and analyzed directly (lane 7) or after immunoprecipitation with T7·tag antibody (lane 8) by SDS–PAGE.

as described (Higgy *et al.*, 1994) using 2 μg of spermatid mRNA in a 50-μl reaction.

Immunoprecipitation experiments were carried out as described previously (Shao *et al.*, 1997) using either T7·Tag monoclonal antibody (Novagen) or anti-800 antisera (described below) as indicated.

RNA Analysis

Isolation of RNA from tissues and elutriated rat male germ cells and Northern blot hybridization were performed as described previously (Shao *et al.*, 1997).

DNA Sequence Analysis

cDNA inserts from either pGAD/cDNA plasmids or λgt11/cDNA phages were subcloned into pBluescript II KS$^+$. Nucleotide sequences were determined using a cycle sequencing kit (Applied Biosystems) which follows a dideoxy dye-labeling method. Samples were processed on an automated DNA sequencer (Applied Biosystems) in the DNA Sequencing Facility at the University of Calgary. The Spag4 cDNA sequence was deposited at GenBank (Accession No. AF116535). Nucleotide and protein sequence analysis was done using the OMIGA program (Oxford Molecular Ltd.).

Generation of 55-800 Deletion Mutants

A schematic diagram of all deletion mutants is presented in Fig. 5. Each cDNA fragment was cloned into pGAD424 (Clontech) in frame with the GAL4 transactivation domain as follows. The fragment 82-800 was obtained by a polymerase chain reaction (PCR) using the LeuMu oligonucleotide (5′ GAGGAATTCCAGCAGCTCCAGG 3′) and T3 oligonucleotide (5′ ATTAACCCTCACTAAAG 3′) as primers and pBSIIKS+/55-800 as template. The PCR product was digested with *Eco*RI and *Sal*I and cloned into the corresponding sites of pGAD424, generating pGAD/82-800. pGAD/82-800 was digested with *Sma*I and *Sal*I, with the larger fragment gel purified, made blunt-ended, and self-ligated, generating pGAD/82-494. Similarly, pGAD/82-800 was digested with *Sac*I and *Sal*I, with the larger fragment gel purified, made blunt-ended, and self-ligated, generating pGAD/82-218. pGAD/1-494 and pGAD/1-218 were constructed in a similar way using the *Sac*I and *Sal*I sites, respectively, using pGAD/800 plasmid as a starting point. For the construction of pGAD/del(82-218), fragment 1-82 was obtained by PCR using oligonucleotide GAL4 TAD (5′ ATAGCGGCCGCGTTTGGAATCACTACAG 3′) and oligonucleotide 800 Leu antisense (5′ TGTGAGCTCAGTTGCTGGCCCTG 3′) as primers and pGAD/800 as template, and the PCR product was digested with *Eco*RI and *Sac*I. pGAD/800 was digested with *Eco*RI and *Sac*I and the larger fragment was gel purified. The above two fragments were ligated, resulting in pGAD/Δ(82-218), harboring fragment 218-800 linked in frame to fragment 1-82. To construct the leucine zipper deletion mutant pGAD/134-800, we used 800 LZ del oligonucleotide (5′ GAGGAATTCGTTCGTGCAGCCCACAGTGA 3′) and the T3 oligonucleotide as primers and pBS/800 as template to PCR, the 134-800 fragment. The PCR product was digested with *Eco*RI and *Sal*I and cloned into the corresponding sites of pGAD/424 in frame with the GAL4 transactivation domain. To generate the pGAD/Δsad1 plasmid the fragment upstream of the sad1 homology region was obtained by PCR using the 800 SAD1del primer 1 (5′ ACA**GGATCC**TGGGCGGGCGTAGTTCCAGA 3′; *Bam*HI site is in boldface) and GAL4-TAD primer and pGAD/800 as template in PCR. The PCR product was digested with *Eco*RI and *Bam*HI. The fragment downstream of the sad1 homology region was obtained by PCR using the oligonucleotides 800SAD1del primer 2 (5′ AGA**GGATCC**ACCGGAGGAGCCAGCAGTG 3′; *Bam*HI site is underlined) and M13 reverse primer and pBS/800 as template in PCR. The product was digested with *Sal*I

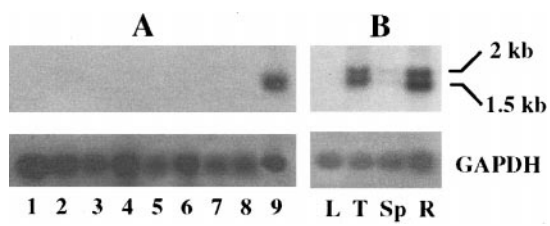

FIG. 2. Spermatid-specific expression of the novel gene. (A) The expression pattern of Spag4 was investigated in various mouse tissues and organs by Northern blot analyses using the insert of pGAD/55-800 as a probe (top): (1) kidney, (2) ovary, (3) liver, (4) brain, (5) lung, (6) small intestine, (7) spleen, (8) thymus, (9) testis. (B) RNA was isolated from purified fractions of pachytene spermatocytes (lane Sp) and round spermatids (lane R) and was subjected to Northern blot analyses using the same pGAD/55-800 probe (top). Gels were run longer to resolve different RNA species. Lanes L and T contained RNA isolated from total liver and testis, respectively. Two transcripts of 2 and 1.5 kb were detected. Filters were stripped and rehybridized using a glyceraldehyde-3-phosphate dehydrogenase cDNA (GAPDH) to confirm loading and quality of RNAs (bottom).

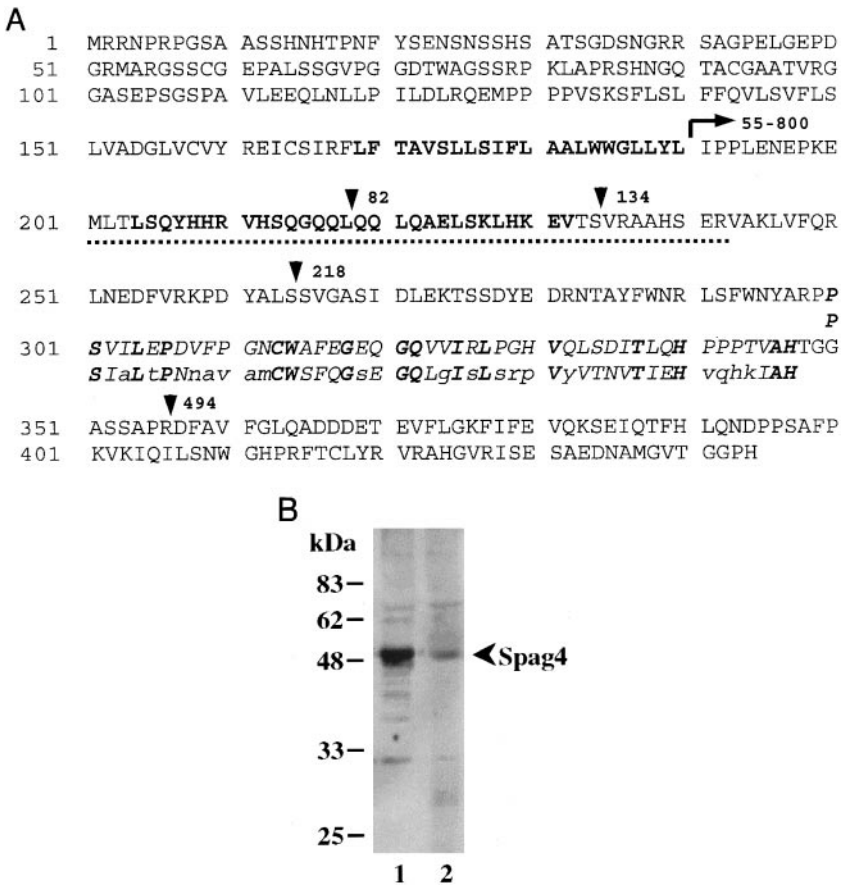

FIG. 3. Amino acid sequence of Spag4. (A) Full-length Spag4 cDNA was sequenced and the predicted amino acid sequence is shown. The fragment contained in clone pGAD/55-800 is indicated (55–800). The region predicted to fold as coiled coil is indicated with a broken underline. Two potential leucine zipper motifs, of which only the downstream one was present in the interacting clone pGAD/55-800, are indicated in boldface. The Spag4 sequence from residues 300–347 is shown in a comparison with residues 360–397 from sad1: identical residues are in boldface, italic capitals; conserved changes are in italic capitals; and different residues are in italic, lowercase letters. Also indicated are breakpoints of mutants described in the text. (B) Full-length Spag4 cDNA clone 800-F and spermatid mRNA was translated *in vitro*. The *in vitro* translation mixtures were immunoprecipitated using anti-800 antisera and analyzed by SDS–PAGE (lanes 1 and 2, respectively). The 49-kDa Spag4 protein is indicated.

and *Bam*HI. The above two fragments were ligated together with the *Eco*RI and *Sal*I digested pGAD424, generating pGAD/Δsad1. Production of all wild-type and mutant proteins in yeast was confirmed by Western blot analysis.

Antibody Preparation

The cDNA insert of pGAD/55-800 was cloned as an *Eco*RI–*Sal*I fragment in pMAL-c2, in frame with the MBP protein, generating pMBP-800. The MBP-800 fusion protein was expressed in TB1 bacteria, purified using amylose–agarose beads (Sigma), and used to generate polyclonal antisera in New Zealand White rabbits. Antisera were characterized by Western blot and immunoprecipitation assays and affinity-purified using nitrocellulose-immobilized MBP-800 fusion protein as described before (Oko and Maravei, 1994).

Protein Localization

Microscopic immunocytochemistry. Rat testis isolation and fixation, preparation of 5-μm paraffin-embedded sections, and antibody incubations were as described previously (Oko, 1998). Affinity-purified antiMBP-800 antiserum served as primary antibody and the secondary antibody was peroxidase-conjugated goat anti-rabbit IgG. After immunoperoxidase reactions, sections were counterstained in 0.1% methylene blue.

Electron microscopic immunocytochemistry. Procedures have been described (Shao *et al.*, 1997; Oko, 1998). Affinity-purified anti-MBP-800 protein antiserum was used as primary antibody, and colloidal gold-conjugated goat anti-rabbit IgG was the secondary antibody.

RESULTS

Isolation of a Novel Odf1-Interacting Protein

Using a yeast two-hybrid screen to isolate proteins that interact with the Odf1 leucine zipper, we previously reported the cloning and characterization of Odf2 (Shao *et al.*, 1997).

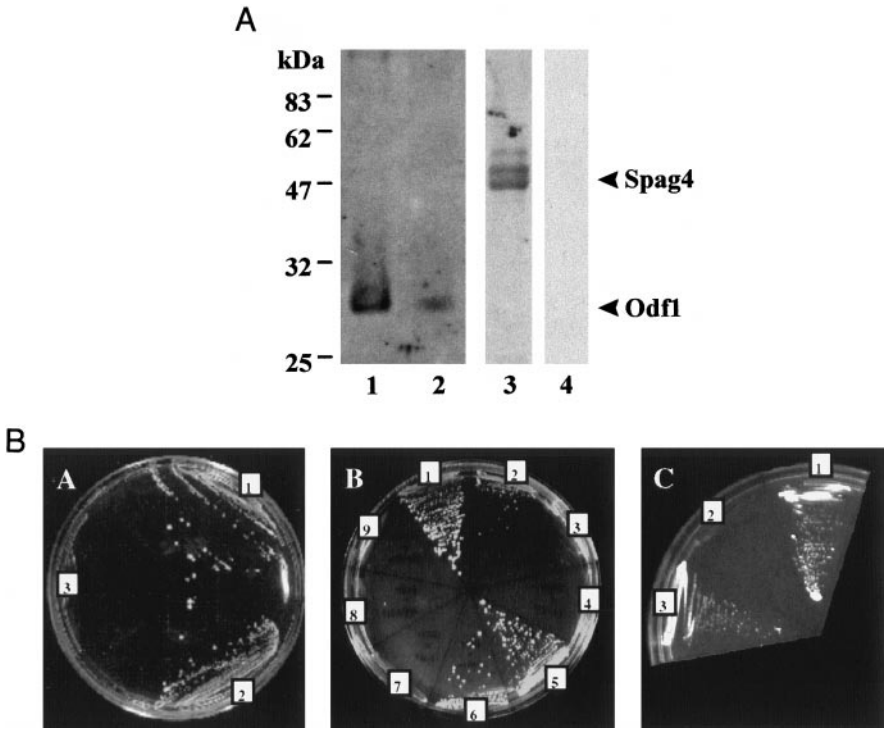

FIG. 4. Spag4–Odf1 complexes in spermatids and yeast. (A) Protein extracts were prepared from purified elongating rat spermatids and complexes were immunoprecipitated using anti-Odf2 antisera (lanes 1 and 4), anti-Spag4 antisera (lane 2), and anti-Odf1 antisera (lane 3). Complexes were resolved by SDS–PAGE and transferred to filters by Western blot procedures, and their composition was analyzed using anti-Odf1 antisera (lanes 1 and 2) and anti-Spag4 antisera (lanes 3 and lane 4). (B) Panel A: To determine if the Odf1 leucine zipper is involved in the interaction with Spag4, pGBT/Odf1NT (1), pGBT/Odf1NT100 (2), and pGBT/Odf1NTdelLZ (3), which contain fragments of residues 1–147, 1–100, and 35–147, respectively, were cotransformed with pGAD/55-800 into yeast. Note that pGBT/Odf1NTdelLZ lacks the leucine zipper motif. Panel B: Regions in Spag4 involved in interaction with Odf1 were analyzed using various pGAD/55-800 deletion mutants (described in the text) in yeast cotransformed with pGBT/Odf1NT: (1) pGAD/55-800, (2) mutant 82-800, (3) 82-494, (4) mutant 82-218, (5) mutant 1-494, (6) mutant Δsad1, (7) mutant 1-218, (8) mutant Δ82-218, (9) mutant 134-800. Results are summarized in Fig. 5. Panel C: Interaction of Spag4 and Odf2 was analyzed in yeast: (1) pGBT-Odf1NT + pGAD/55-800, (2) pGBT-Odf2 + pGAD/55-800, (3) pGBT-Odf1NT + pGAD-Odf2.

Here, we characterize a second group of Odf1-interacting cDNA clones. The largest of these had an insert of 800 bp and was designated pGAD/55-800. The interaction between the novel protein encoded by pGAD/55-800, which we call Spag4, and Odf1 was verified using *in vitro* translation and coimmunoprecipitations. To this end we cloned the cDNA insert of pGAD/55-800 in pBS-ATG (Shao *et al.*, 1997), which provides an in-frame initiation codon for *in vitro* translation. The resulting plasmid, pBS-ATG/800, and pET/RT7NT, which contains Odf1NT fused to an S10 epitope tag (Higgy *et al.*, 1994), were *in vitro* transcribed and translated individually and each translation mixture was immunoprecipitated with T7·tag antibody, which recognizes the S10 epitope tag. As expected, the antibody specifically and efficiently immunoprecipitates S10 epitope-tagged Odf1NT, but not Spag4 (Fig. 1, lanes 6 and 4, respectively). pBS-ATG/800 and pET/RT7NT were next cotranslated (Fig. 1, lane 7) and immunoprecipitated using T7·Tag antibody. The results show that Spag4 efficiently coimmunoprecipitates with epitope-tagged Odf1NT (Fig. 1, lane 8). These results demonstrate that Spag4 interacts efficiently with Odf1 *in vitro*, confirming the interaction originally identified in yeast.

Spag4 mRNA Is Exclusively Expressed in Spermatids

Odf1 is transcribed exclusively in round spermatids and its translation is initiated in elongating spermatids. To analyze whether the newly identified Odf1-interacting protein Spag4 is physiologically related to Odf1 in male germ cells, we performed Northern blot analyses to examine its expression pattern in different tissues of the mouse. The results show that the novel gene is detectably expressed only in mouse testis and not in other tissues tested, including kidney, ovary, liver, brain, lung, small intestine, spleen, and thymus (Fig. 2A). The RNA expression pattern

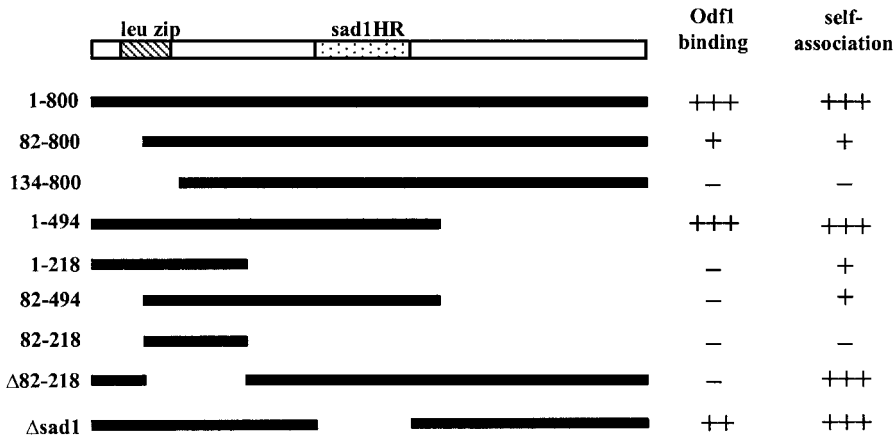

FIG. 5. Summary of protein–protein interaction studies in yeast. Indicated are the location of the leucine zipper motif and the region with similarity to the yeast spindle pole body protein sad1 on the Spag4 protein fragment present in clone pGAD/55-800. Bars indicate the sequences retained in the various Spag4 deletion mutants. Efficiency of binding of Spag4 to Odf1 and to itself is indicated on a relative scale based on the number of yeast colonies detected in experiments similar to those shown in Figs. 4 and 6. Note that mutant Δ82-218, which lacks the 3′ half of the leucine zipper motif, does not bind to Odf1, but supports Spag4 self-association as efficiently as wild-type Spag4.

was further investigated in purified male germ cells (pachytene spermatocytes and round spermatids) isolated by centrifugal elutriation using Northern blot analysis. The result shows that the novel gene, Spag4, is exclusively transcribed in round spermatids (Fig. 2B, lane R). Two RNA transcripts were detected in spermatids: a 1.5-kb RNA and a 2-kb RNA. Further analysis presented below suggests that the 1.5-kb RNA is the mature Spag4 mRNA. The larger species could represent an mRNA precursor or may result from use of an alternative, downstream polyadenylation signal. Therefore, Spag4 expression is spermatid specific, a pattern identical to that of Odf1.

Spag4 Harbors Leucine Zipper Motifs

To obtain full-length cDNAs we screened a λgt11 testicular cDNA library. Two cDNA clones were obtained with insert sizes of approximately 0.85 and 1.5 kb and were named 800-A, and 800-F, respectively. Further cDNA cloning was carried out using a 5′ RACE (rapid amplification of cDNA end) method; however, no further sequences upstream of the 5′ end of 800-F cDNA were obtained. When the 1.5-kb fragment of clone 800-F was used as a probe in Northern blot hybridization, two transcripts of 2.0 and 1.5 kb were detected (not shown). The nucleotide sequence of the cDNA inserts of these clones was determined (GenBank Accession No. AF116535): the deduced Spag4 amino acid sequence is shown in Fig. 3A. The partial cDNA fragment present in clone pGAD/55-800 is indicated. A GenBank search revealed only one protein, the yeast sad1 protein (Hagan and Yanagida, 1995; GenBank Accession No. X85105), with significant similarity in a small region of Spag4. Spag4 residues 300–347 have 62% sequence similarity with sad1 residues 360–407 (33% of residues are identical and a further 29% are conservative substitutions). No gaps are required for alignment (Fig. 3A, italicized letters). Mutation of sad1, a microtubule-binding protein, results in disruption of spindle assembly in yeast (Hagan and Yanagida, 1995). Interestingly, this same region (which we designate sad1 homology region, sad1HR) also carries the σ^{54}-interaction domain signature, an ATP-dependent protein interaction domain (Prosite Database). Computer analysis shows that two putative leucine zippers are present in Spag4 (Fig. 3A, boldface letters), as is a region predicted to fold as a coiled coil (broken underline). The latter region encompasses the leucine zipper present in clone pGAD/55-800, but not the upstream putative leucine zipper. The two leucine zippers are separated by a short stretch of amino acids rich in proline residues.

Spag4 Encodes a 49-kDa Spermatid Protein

To analyze the coding capacity of full-length Spag4 cDNA 800F, we carried out *in vitro* translations followed by immunoprecipitation using anti-800 antisera. As shown in Fig. 3B, 800F cDNA encodes a protein with an apparent molecular weight of 49,000 (lane 1) identical to the expected size (49 kDa). Smaller products likely arise from internal translation starts. To determine the size of the product encoded by Spag4 in spermatids, mRNA was isolated from elutriated, round spermatids and translated in a reticulocyte lysate system. Spag4 protein was immunoprecipitated using anti-800 antisera. The result (Fig. 3B, lane 2) shows that Spag4 mRNA directs synthesis of a protein with an apparent molecular weight of 49 kDa, which comigrates with the *in vitro* translation product of 800-F cDNA. We conclude from these data that Spag4 encodes a 49-kDa spermatid-specific protein.

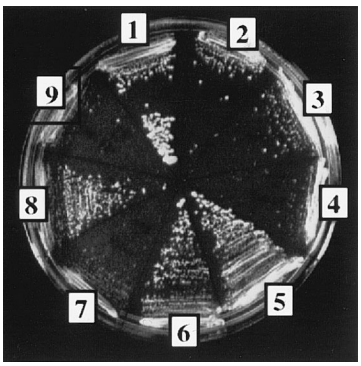

FIG. 6. Sequences involved in Spag4 self-interaction. Spag4 deletion mutants were constructed from pGAD/55-800 and analyzed for their ability to interact with wild-type Spag4 in yeast cotransformed with pGBT/55-800: (1) pGAD/55-800, (2) mutant 82-800, (3) 82-494, (4) mutant 82-218, (5) mutant 1-494, (6) mutant Δsad1, (7) mutant 1-218, (8) mutant Δ82-218, (9) mutant 134-800. Results are summarized in Fig. 5.

Spag4 and Odf1 Interact in Spermatids

The data presented above, including the interaction in yeast and *in vitro* and the expression pattern, strongly suggested that Spag4 and Odf1 specifically interact and that this interaction is physiologically relevant. To confirm this interaction *in vivo* we analyzed Odf1–Spag4 complexes in elongating spermatids. Proteins were extracted from elutriated, purified rat elongating spermatids and Odf1–Spag4 complexes were analyzed in immunoprecipitation assays followed by Western blot analysis of the precipitated complexes. Anti-Odf1 and anti-800 antisera were used in both combinations. We also analyzed the presence of potential Odf1–Odf2 complexes and Odf2–Spag4 complexes using anti-Odf2 antibodies in immunoprecipitations. The results (Fig. 4A) show that anti-Odf2 and anti-800 antibodies immunoprecipitate protein complexes in spermatids that contain Odf1 (lanes 1 and 2, respectively). The smaller amount of Odf1 complexed to Spag4 reflects the smaller quantities of Spag4 protein compared with Odf2 in these cells. As expected from this result, complexes immunoprecipitated with anti-Odf1 antibodies contain Spag4 (lane 3). However, we were unable to detect complexes that contain Odf2 and Spag4 (lane 4), which is in agreement with similar results in yeast (see below). Our data suggest that Odf1 and Spag4 either interact directly *in vivo,* a conclusion supported by our yeast and *in vitro* results, or are part of a larger protein complex.

The Spag4 Leucine Zipper Mediates Interaction with Odf1

We determined that Odf1 interacts with Spag4 and that Spag4 likely contains leucine zipper motifs (Fig. 3A). To determine whether the Odf1 leucine zipper is involved in the interaction with Spag4 protein, we tested the interaction of pGAD/55-800 with three Odf1 fragments in yeast: pGBT/Odf1NT, pGBT/Odf1NT100, and pGBT/Odf1NTdelLZ

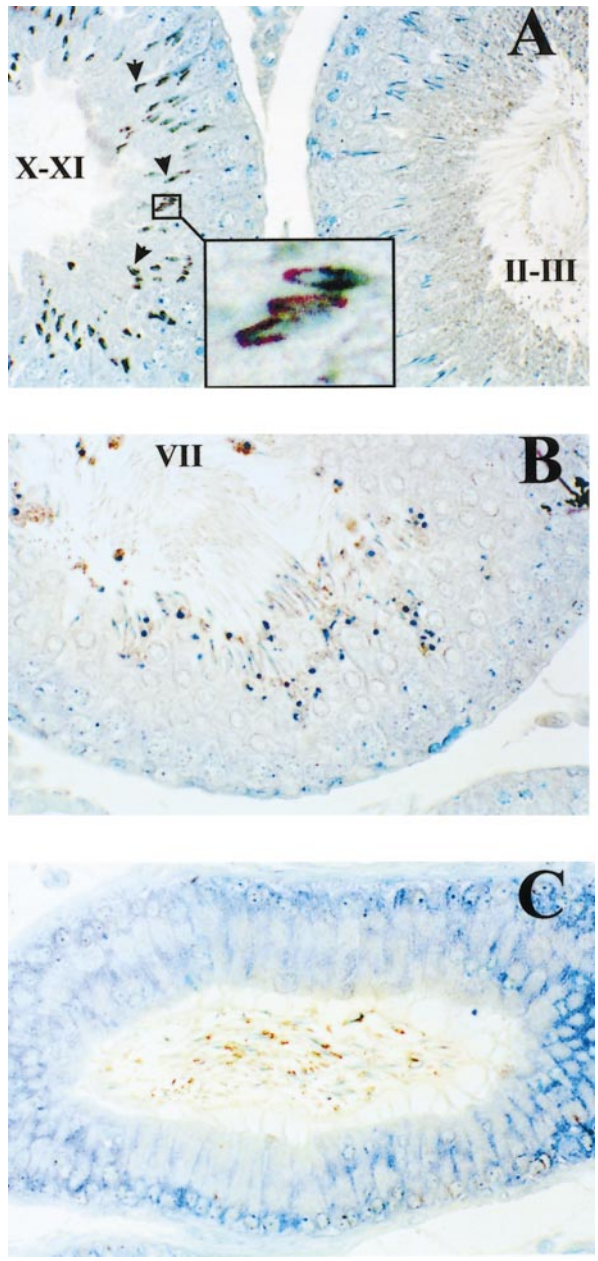

FIG. 7. Spag4 localizes to spermatid manchette and tail. Light micrographs of portions of seminiferous tubules in different, indicated, stages of the cycle of the rat seminiferous epithelium immunoperoxidase-stained with affinity-purified anti-800 antisera. Immunoperoxidase reaction products are evident over the manchette (A, stage X–XI, arrowheads) and tails of spermatids at stages II–III (A) and VII (B), and of epididymal sperm (C). The inset in (A) shows an enlargement of the indicated area.

(which lacks the leucine zipper motif). The results (Fig. 4B, panel A) show that Odf1 fragments containing the leucine zipper interact efficiently with Spag4, whereas the Odf1 fragment lacking the leucine zipper motif fails to interact with Spag4. We conclude that, interestingly, these data show that the Odf1 leucine zipper can bind specifically to more than one protein, viz., Spag4 and Odf2.

To delineate the Spag4 sequence(s) involved in interaction with Odf1, Spag4 deletion mutants were tested in yeast. The results are shown in Fig. 4B, panel B, and summarized in Fig. 5. Deletion of a portion of the leucine zipper plus flanking sequences in pGAD/55-800 (mutant 82-800) greatly reduced Spag4–Odf1 association, and deletion of the entire leucine zipper (mutant 134-800) completely abolished interaction. This demonstrated that the leucine zipper contained within the predicted coiled-coil region (Fig. 3A) is required for the interaction of Spag4 with Odf1. Other constructs were tested to uncover contributions of additional Spag4 sequences in the interaction with Odf1. Deletion of the 88 C-terminal residues (mutant 1-494) had no effect, but further deletion of another 98 residues (mutant 1-218) abolished interaction, even though this mutant retains all of the leucine zipper and thirty 3′-flanking amino acids. A similar result had been observed previously for Odf1 (Shao and van der Hoorn, 1996), suggesting that sequences flanking the leucine zipper are involved in the interaction. Since mutant 1-494, but not mutant 1-218, harbors the sad1HR (Fig. 3A), it was possible that this sequence was involved in association of Spag4 and Odf1. We tested this possibility using a sad1HR deletion mutant, Δsad1, which lacks residues 300–347. Deletion of sad1HR resulted in only a small reduction in Odf1 association.

To further define the specificity of the leucine zipper-mediated interactions described above we investigated whether Spag4 can interact in yeast with Odf2. Figure 4B, panel C, shows that Spag4 and Odf2 do not interact despite the presence of leucine zippers in these two proteins. This result corroborates our failure to identify Spag4–Odf2 complexes in spermatids (Fig. 4A) and underscores the specificity involved in the interactions of Odf1 and Spag4 and Odf1 and Odf2 (Shao *et al.*, 1997).

Spag4 Can Self-Associate

While carrying out the experiments described above, we observed that Spag4 protein efficiently self-interacts. To determine the involved region, we used Spag4 mutants shown in Fig. 5 and examined their interaction with wild-type Spag4. The results are shown in Fig. 6 and summarized in Fig. 5. A deletion in mutant Δ82-218, which removes half of the Spag4 leucine zipper and abolishes leucine zipper-mediated association of Spag4 with Odf1 (Fig. 4), had no effect on self-interaction, indicating that the leucine zipper is not directly involved in self-interaction. Similarly, neither sad1HR nor the C-terminal 88 residues are involved in self-interaction. However, self-interaction is largely abolished by further deletion from the C-terminal end (mutant 1-218). Deletion of the 28 N-terminal residues encoded by pGAD/55-800 significantly reduced self-interaction, as shown by mutants 82-800 and 82-494. These data suggest that two nonlinked regions are involved in self-interaction (see Fig. 3A): (1) amino acid residues 191–219 and (2) 35 amino acids from 265 to 300. Our results also suggest that the sad1HR sequence does not play an important role in interaction of Spag4 with Odf1 or itself.

Spag4 Binds to Microtubules in Elongating Spermatids

Odf1 protein accumulates in ODF of late elongating spermatids and is present in ODF of epididymal sperm. The other major ODF protein, Odf2, with which Odf1 interacts specifically via leucine zippers has a protein expression pattern indistinguishable from that of Odf1 (Shao *et al.*, 1997; Schalles *et al.*, 1998). To investigate Spag4 protein expression we prepared rat testis sections and analyzed Spag4 protein by immunocytochemistry using affinity-purified anti-800 antiserum. The results are shown in Fig. 7. Spag4 protein expression starts in step 10 spermatids. Unexpectedly, in these cells the protein localizes to the manchette, a transient structure consisting of microtubules that encircle the condensing nucleus (Fig. 7A, arrowheads, and inset, which shows enlargement of indicated area). At later stages of spermatid development (steps 16–17, Fig. 7A) Spag4 is detectable in the developing sperm tail. Figure 7B shows staining of tails of step 18–19 spermatids. Spag4 reactivity remains associated with the tail in epididymal sperm (Fig. 7C). Since Spag4 is detectable in both the midpiece and principal piece of elongating spermatids (Figs. 7A and 7B) the protein is likely a component of ODF and/or the axoneme, which are present throughout the sperm tail. To identify sperm tail structures that contain Spag4, and to analyze which component of the manchette contains Spag4, immunogold electronmicroscopy was performed on rat testis sections using affinity-purified anti-800 antisera. The analysis of the association of Spag4 with the manchette is shown in Fig. 8. Spag4 is first detectable in association

FIG. 8. Spag4 protein localization on manchette microtubules. Spag4 was detected in sections of rat testes by immunogold electronmicroscopy using affinity-purified anti-800 antibodies. (A) Micrograph showing Spag4 reactivity over microtubules of the manchette mantle surrounding the periaxonemal compartment in step 10 spermatids (arrows). Also visible is Spag4 over the axoneme at this stage (arrowheads). (B) Spag4 reactivity is seen over the manchette in step 12 spermatids (inset shows an enlarged view of a part of the manchette). (C) Spag4 labeling is evident over the manchette microtubules of step 10–11 spermatids in the cross section shown. ×38,000.

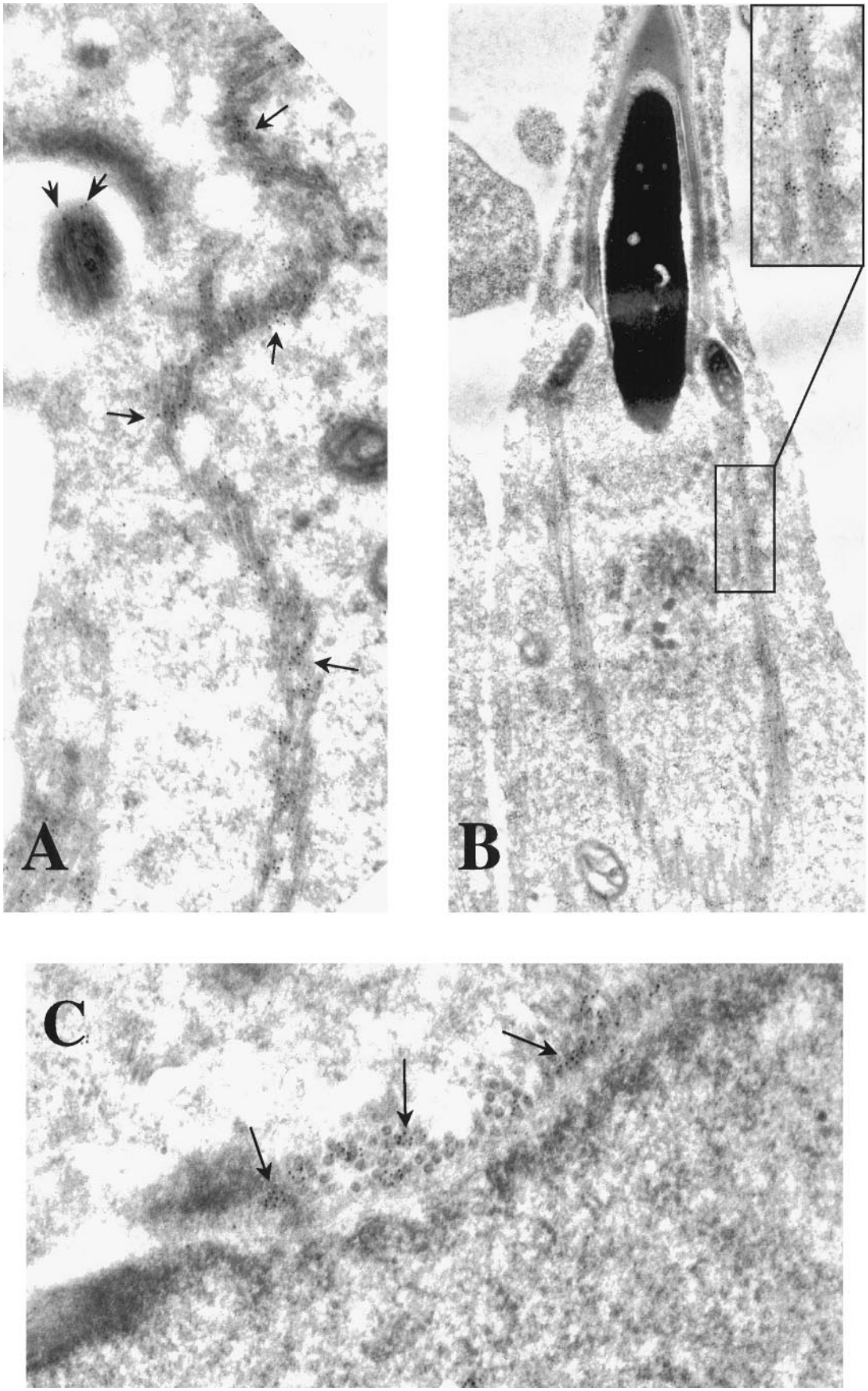
A
B
C

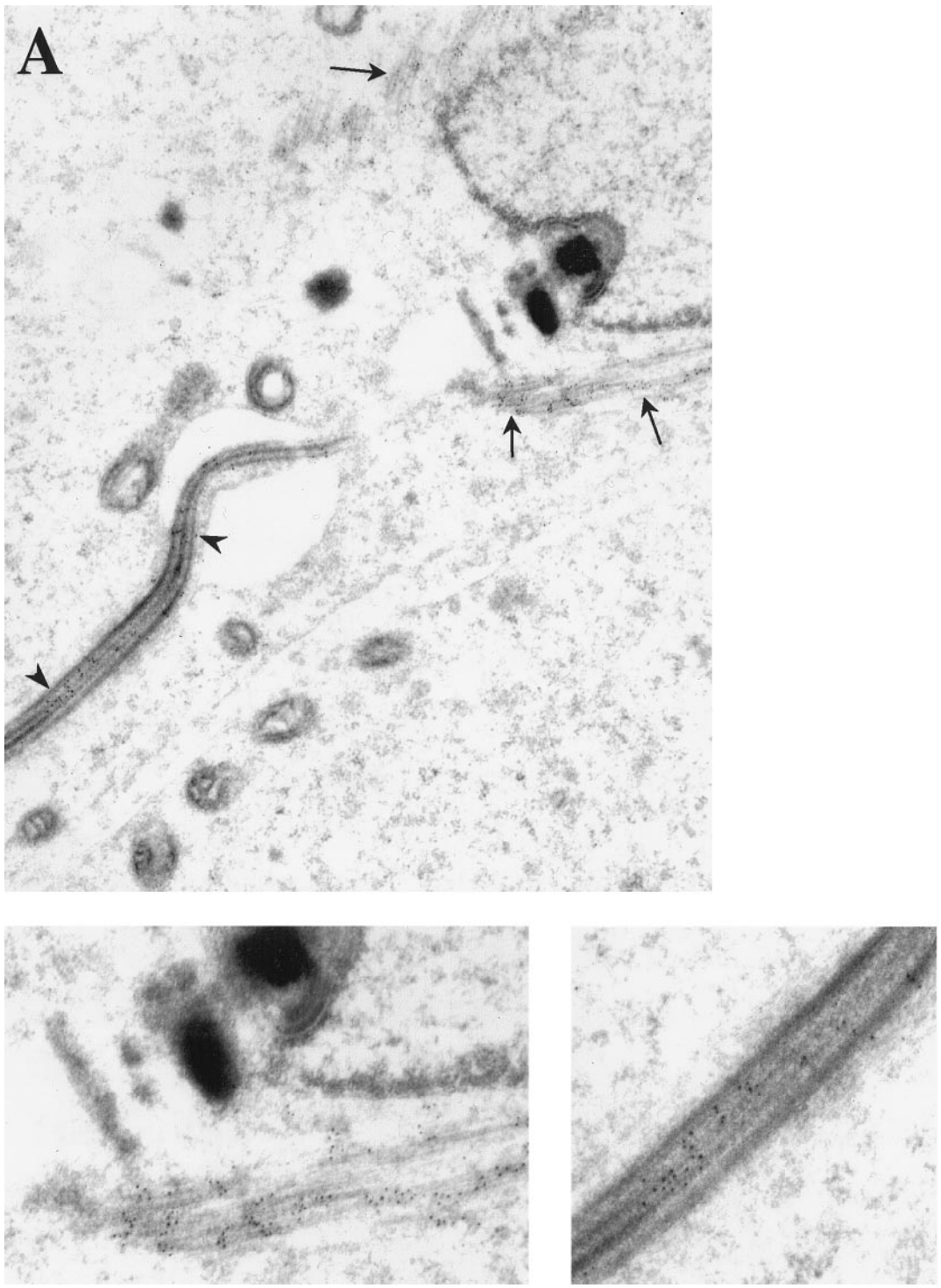

FIG. 9. Association of Spag4 with the axoneme. (A) Micrograph showing Spag4 reactivity over step 9–10 spermatid axoneme (arrowheads) and manchette (arrows) using methods described above. Spag4 localizes exclusively to the microtubules in these cells that have just started ODF assembly. Two areas are shown enlarged for ease of viewing gold label. (B) In step 15 spermatids Spag4 labeling is over the axonemal microtubules (arrows). No labeling of mitochondria and annulus (arrowheads) was detected. The inset shows an enlarged area of the forming midpiece: note that label is not associated with the electron-dense ODF, but exclusively with the axoneme. (C) Micrograph showing Spag4 reactivity over the axoneme in the midpiece of step 18–19 spermatids (arrows) in a longitudinal section. Note the lack of signal over the ODF and mitochondria. (D) Cross sections through the principal piece of step 14–15 spermatids show that Spag4 reactivity is confined to the axoneme: no label is present over the FS. ×35,000.

FIG. 9—*Continued*

with both the manchette and axoneme in step 10–11 spermatids: Figure 8A shows Spag4 on manchette microtubules (arrows) surrounding the periaxonemal compartment and the axoneme (arrowheads). Spag4 is also clearly detectable on manchette microtubules of step 12 spermatids (Fig. 8B). At this stage of spermatid development, the apical part of the nucleus is condensed and the manchette is attached to the nuclear ring (Fig. 8B). Figure 8C shows Spag4 labeling over and around manchette microtubules (arrows) in a cross section through step 10–11 spermatids. These data demonstrate that Spag4 associates with microtubules of the manchette mantle. This suggested the intriguing possibility that Spag4 also associates with axonemal microtubules in spermatids rather than with ODF, the site of Odf1. This possibility was investigated and results are shown in Fig. 9. First, Spag4 can be detected in step 9–10 spermatids on the axoneme (Fig. 9A). In these cells, Odf1 and Odf2 expression and ODF assembly have just begun. Interestingly, in the

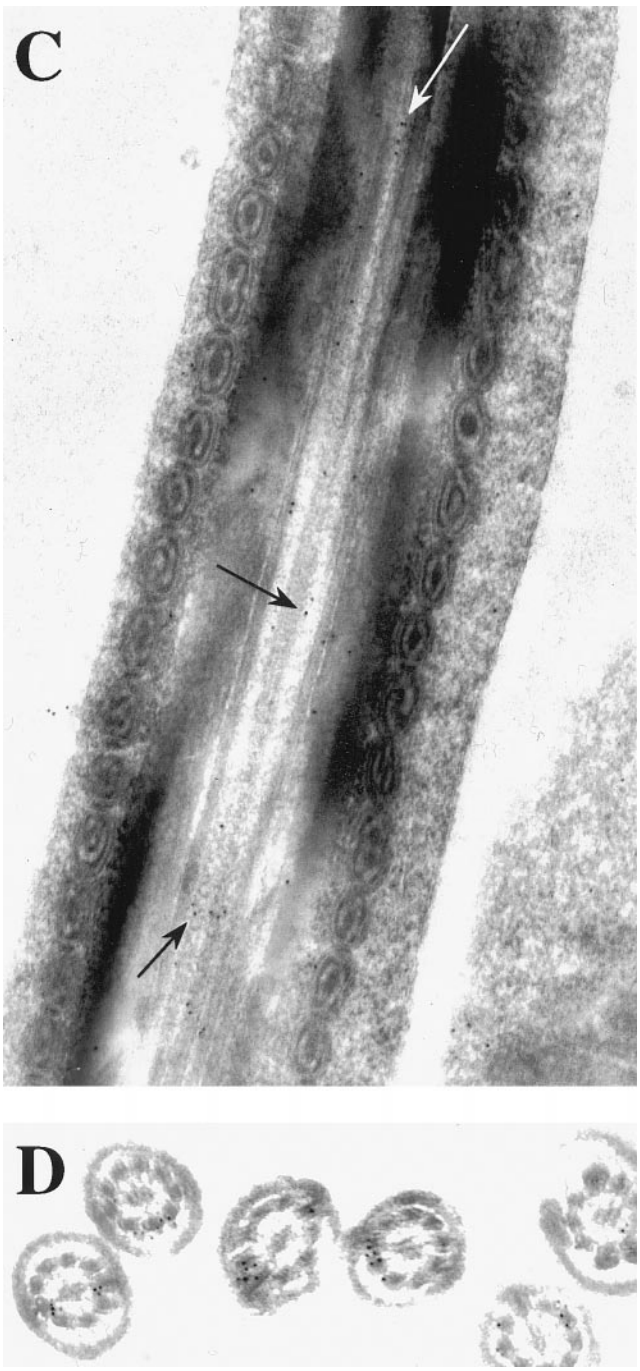

FIG. 9—*Continued*

section shown in Fig. 9A, labeling of Spag4 can be seen over microtubules of both the axoneme and the manchette (arrowheads and arrows, respectively). Two areas are enlarged to demonstrate Spag4 reactivity. Later, in step 15 spermatids, labeling is over the axoneme, not over ODF or FS (Fig. 9B, arrows): visible in this micrograph are also the annulus (arrowheads), which has descended, and mitochondria that line up to form the midpiece. Neither of these structures contains detectable Spag4. Figure 9C shows a longitudinal section through the midpiece of a step 18–19 spermatid, which represents the last stage before release into the lumen of the seminiferous tubule: Spag4 is associated only with the axoneme (arrows), not with mitochondria or ODF. Figure 9D shows a composite of cross sections through the principal piece of sperm tails of step 14–15 spermatids: labeling is exclusively on the axoneme. Our data show that Spag4 is associated with microtubules throughout spermiogenesis, and suggest the possibility that Spag4 is a microtubule-binding protein.

DISCUSSION

Protein Interactions in the Sperm Tail

Mammalian sperm tails contain, besides the axoneme unique structures, ODFs and FS, which are formed during spermiogenesis (Oko, 1998). A definite role for ODFs and FS remains to be established but could be in motility or elastic recoil (Baltz *et al.*, 1990). Clearly, to produce a functional tail, the formation of the axoneme, ODFs and FS must be coordinated and previous studies have described their morphogenesis: ODFs grow in a proximal-to-distal orientation, whereas FS grows from the tail tip toward the nucleus. Another important difference between ODFs and FS is that FS is present only in the sperm tail principal piece, whereas ODFs are present in the connecting piece, the midpiece, and the principal piece. Thus, another role for ODFs, besides those mentioned above, may be as anchor for different components in the tail. This predicts that proteins in ODFs interact with axoneme, FS, and/or mitochondria. We and others had previously cloned and characterized two major ODF proteins, Odf1 (van der Hoorn *et al.*, 1990; Burfeind and Hoyer-Fender, 1991; Morales *et al.*, 1994) and Odf2 (Shao *et al.*, 1997; Brohmann *et al.*, 1997; Turner *et al.*, 1997). Their role in ODF morphogenesis and function is not known. However, we recently demonstrated that (i) these two proteins interact specifically using leucine zipper motifs (Shao *et al.*, 1997) and (ii) their sub-ODF localization differs. Odf1 and Odf2 are both present in the medulla. However, whereas Odf1 is on the surface of ODFs that face the axoneme, Odf2 is present in the cortex and consequently faces mitochondria in the midpiece and FS in the principal piece (Schalles *et al.*, 1998). Therefore, the possibility exists that Odf1 and Odf2 not only provide a molecular network for ODF but may also functionally interact with different proteins present on other tail components.

Leucine Zippers Are a Major Determinant of Sperm Tail Protein Interactions

Here we describe the cloning and characterization of a novel 49-kDa protein, Spag4, which is the first identified candidate for such an interacting non-ODF partner. Spag4 is

a leucine zipper-containing protein that is specifically expressed in spermatids. Spag4 strongly interacts with Odf1, but not Odf2, as detected both *in vitro* and *in vivo*. Spag4 also appears to self-associate.

Spag4 was cloned as a protein that interacts with the N-terminal half of Odf1 in a yeast two-hybrid screen. Sequence analysis of this clone predicted the presence of a leucine zipper motif contained within a region predicted to fold as a coiled coil. Our deletion studies in yeast demonstrate that the Spag4 region containing this motif indeed interacts with the Odf1 leucine zipper. However, Spag4 residues downstream of the leucine zipper contribute also to this interaction: deletion of the region from residues 265 to 300 markedly decreased the efficiency of interaction with Odf1. Deletion of the flanking residues (300–347) that are similar to a sequence in the yeast sad1 protein (see below) had only a small effect.

The results presented here together with our previous data (Shao and van der Hoorn, 1996; Shao *et al.*, 1997) have uncovered a remarkable specificity in the leucine zipper-mediated interactions of sperm tail proteins that is reminiscent of the situation described for members of the Fos and Jun families of transcription factors. The Odf1 leucine zipper mediates specific interactions with Odf2 and with Spag4. Spag4 does not, however, interact with Odf2. We recently cloned another testis-specific protein, Spag5, which also strongly interacts with Odf1, but not Odf2, via a leucine zipper (Shao and van der Hoorn, in preparation). The molecular basis for the ability of the Odf1 leucine zipper to recognize at least three partners is not known, but control interaction experiments using bZIP-containing proteins indicated that these cannot associate with Odf1 (Shao and van der Hoorn, unpublished results). The yeast interaction studies also suggested that Spag4 efficiently self-associates. The deletion experiments described here demonstrate that the leucine zipper motif is not involved in self-association (mutant Δ82-218). Two regions contribute to self-association: a stretch of 28 residues flanking and overlapping the leucine zipper at its 5′ end, and a sequence of residues from 265 to 300. Therefore, the sequences that are involved in self-association and those that mediate binding to Odf1 partially overlap. It is possible that these two regions are in close proximity in the protein, but proof awaits structure resolution. The functional significance of Spag4's ability to multimerize is unclear.

Spag4 Associates with Spermatid Microtubules

In this study, we discovered that although Spag4 and Odf1 interact, they localize to different spermatid structures. Our immunohistochemical studies using rat testis sections show that Spag4 protein is detectable in step 10 elongating spermatids in a transient structure known as the manchette. At later stages of spermiogenesis, with the disappearance of the manchette, that signal decreases and Spag4 is found associated with sperm tails. The manchette consists of a perinuclear ring, the microtubule mantle, and dense plaques at the distal ends of the mantle (Tres and Kierszenbaum, 1996, and references therein). No definite function has been described for the manchette but recently isolation procedures have been reported (Mochida *et al.*, 1998). In that study four major proteins were identified in the manchette: α- and β-tubulin, β-actin, vimentin, and a 62-kDa perinuclear ring protein. A small number of other proteins were also shown to bind the manchette, viz., sak57 (Tres and Kierszenbaum, 1996), a keratin that is also present in spermatocytes (Tres *et al.*, 1996), SPNR (Schumacher *et al.*, 1995, 1998), a microtubule-associated RNA-binding protein expressed in brain, ovary, and testis and rtTBP1 (Rivkin *et al.*, 1997), and a putative ATPase that may function in the 23 S proteasome. Our light microscopic observations were extended by immunogold electronmicroscopic studies: in spermatids, Spag4 is clearly associated with manchette microtubules, not with other manchette structures, and with the axonemal microtubules. Spag4 is not present in other sperm tail structures. This latter finding constitutes an important difference with the manchette-associated proteins mentioned above. Sak57 and rtTBP1 associate at later stages of spermiogenesis with ODFs and with mitochondria and ODFs, respectively, not with the axoneme (Tres and Kierszenbaum, 1996; Rivkin *et al.*, 1997). The binding of Spag4 to microtubules could be either direct or via an unidentified microtubule-associated protein. In this context, the presence of a sequence in Spag4 with high similarity to a region in the yeast sad1 protein (Hagan and Yanagida, 1990) may be significant. Sad1 encodes a 58-kDa spindle pole body protein that is essential for viability: mutation results in most cells unable to form a normal mitotic spindle or formed spindles on which chromosomes failed to separate (Hagan and Yanagida, 1995). Sad1 may interact directly with microtubules and has been proposed to act as an attachment for microtubule motor proteins. Therefore, although sad1 and Spag4 are present in vastly different cell types they both localize to microtubule structures inside the cell and the intriguing possibility exists that the region of similarity that they share constitutes a microtubule binding motif. A function for Spag4 in the manchette remains to be determined.

Spag4 as a Part of a Molecular Link between ODF and Axoneme

Our interaction data show that Spag4 binds Odf1 but not Odf2. In addition, no Odf1–Odf2–Spag4 complex was detectable in spermatids. This suggests that elongating spermatids harbor complexes containing Odf1–Odf2 or Odf1–Spag4. What could be a role for Spag4 in sperm tail development or function? One model is that Spag4 is involved directly in transport of Odf1 to the assembling ODFs in elongating spermatids. We believe that such a role, although theoretically possible, is unlikely since the majority of Odf1 never associates with Spag4, yet is correctly deposited in developing ODF (e.g., as complexes with Odf2). Another possibility, which we favor, is that Spag4 com-

plexes a subset of Odf1 molecules, which can no longer bind Odf2, and subsequently the Spag4–Odf1 complex localizes to the axoneme. Consequently, Odf1 forms the surface of developing ODFs that face the axoneme. In this model, Spag4 is involved in the positioning of developing ODFs by forming a link with Odf1 between ODFs and axonemal microtubules. This model is supported by our data so far including the interaction results and the timing of Spag4 expression (Spag4 is present on the axoneme at the very first stages of ODF assembly) and explains the exclusion of Odf2 from the inner ODF surface (Schalles *et al.*, 1998). Importantly, the model predicts an essential role for axonemal components in the correct formation of ODF structures. Indeed, the analysis of homozygous male sterility-inducing mutation hpy (Bryan, 1977) and of transgenic OVE 219 male mice (Russell *et al.*, 1994) supports this model: spermatids in these mutant mice lack normal axonemes and ODF assembly is abnormal. Abnormal ODFs are found randomly grouped with mitochondria and it has been proposed from these studies that ODF proteins require a normal axoneme as a substrate for their correct assembly and stability.

CONCLUDING REMARKS

Our studies have uncovered the first molecular link between two essential sperm tail structures, ODFs and axoneme. These observations and those of other laboratories will unravel the molecular networks that are the basis for the intricate organization of structures that are unique to the sperm tail. Our current results and previous work also demonstrate the important role of the leucine zipper motif as a mediator of specific sperm tail protein interactions. Together with morphological analyses, this should lead to a deeper understanding of the normal and abnormal sequence of events in the developing sperm tail.

ACKNOWLEDGMENTS

This work was supported by grants from the Medical Research Council of Canada (to R.O. and F.A.v.d.H.) and from the Natural Sciences and Engineering Council of Canada (to R.O.). X.S. was supported by a studentship from the Alberta Heritage Foundation for Medical Research, and J.P.L. was the recipient of an Alberta Heritage Foundation for Medical Research summer studentship award.

REFERENCES

Baltz, J. M., Williams, P. O., and Cone, R. A. (1990). Dense fibers protect mammalian sperm against damage. *Biol. Reprod.* **43,** 485–491.

Brohmann, H., Pinnecke, S., and Hoyer-Fender, S. (1997). Identification and characterization of new cDNAs encoding outer dense fiber proteins of rat sperm. *J. Biol. Chem.* **272,** 10327–10332.

Bryan, J. H. D. (1977). Spermatogenesis revisited. IV. Abnormal spermiogenesis in mice homozygous for another male-sterility-inducing mutation, hpy (hydrocephalic-polydactyl). *Cell Tissue Res.* **180,** 187–201.

Burfeind, P., and Hoyer-Fender, S. (1991). Sequence and developmental expression of a mRNA encoding a putative protein of rat sperm out dense fibers. *Dev. Biol.* **148,** 195–204.

Calvin, H. I. (1979). Electrophoretic evidence for the identity of the major zinc-binding polypeptides in the rat sperm tail. *Biol. Reprod.* **21,** 873–882.

Calvin, H. I., and Bedford, J. M. (1971). Formation of disulfide bonds in the nucleus and accessory structures of mammalian spermatozoa during maturation in the epididymis. *J. Reprod. Fertil. Suppl.* **13,** 65–75.

Calvin, H. I., and Bleau, G. (1974). Zinc–thiol complexes in keratin-like structure of rat spermatozoa. *Exp. Cell Res.* **86,** 280–284.

Carrera, A., Gerton, G. L., and Moss, S. B. (1994). The major fibrous sheath polypeptide of mouse sperm: Structure and functional similarities to the A-kinase anchoring proteins. *Dev. Biol.* **165,** 272–284.

Delmas, V., van der Hoorn, F. A., Mellstrom, B., Jegou, B., and Sassone-Corsi, P. (1993). Induction of CREM activator proteins in spermatids: Down-stream targets and implications for haploid germ cell differentiation. *Mol. Endocrinol.* **7,** 1502–1514.

Fawcett, D. W. (1975). The mammalian spermatozoon. *Dev. Biol.* **44,** 394–436.

Fulcher, K. D., Welch, J. E., Klapper, D. G., O'Brien, D. A., and Eddy, E. M. (1995). Identification of a unique mu-class glutathione *S*-transferase in mouse spermatogenic cells. *Mol. Reprod. Dev.* **42,** 415–424.

Grootegoed, J. A., Grolle-Hey, A. H., Rommerts, F. F. G., and van der Molen, H. J. (1977). Ribonucleic acid synthesis *in vitro* in primary spermatocytes isolated from rat testis. *Biochem. J.* **168,** 23–31.

Hagan, I., and Yanagida, M. (1990). Novel potential mitotic motor protein encoded by the fission yeast *cut7*+ gene. *Nature* **347,** 563–566.

Hagan, I., and Yanagida, M. (1995). The product of the spindle formation gene *sad1*+ associates with the fission yeast spindle pole body and is essential for viability. *J. Cell Biol.* **129,** 1033–1047.

Higgy, N. A., Pastoor, T., Renz, C., Tarnasky, H. A., and van der Hoorn, F. A. (1994). Testis-specific RT7 protein localizes to the sperm tail and associates with itself. *Biol. Reprod.* **50,** 1357–1366.

Irons, M. J., and Clermont, Y. (1982a). Kinetics of fibrous sheath formation in the rat spermatid. *Am. J. Anat.* **165,** 121–130.

Irons, M. J., and Clermont, Y. (1982b). Formation of the outer dense fibers during spermiogenesis in the rat. *Anat. Rec.* **202,** 463–471.

Kuhn, R., Schafer, U., and Schafer, M. (1988). *cis*-Acting regions sufficient for spermatocyte-specific transcriptional and spermatid-specific translational control of the *Drosophila melanogaster* gene (mst3)gl-9. *EMBO J.* **7,** 447–454.

Kuhn, R., Kuhn, C., Borsch, D., Glatzer, K. H., Schafer, U., and Schafer, M. (1991). A cluster of four genes selectively expressed in the male germ line of *Drosophila melanogaster*. *Mech. Dev.* **35,** 143–151.

Lewis, S. A., Ivanov, I. E., Lee, G. H., and Cowan, N. J. (1989). Organization of microtubules in dendrites and axons is determined by a short hydrophobic zipper in microtubule-associated proteins MAP2 and tau. *Nature* **342,** 498–505.

Mochida, K., Tres, L. L., and Kierszenbaum, A. L. (1998). Isolation of the rat spermatid manchette and its perinuclear ring. *Dev. Biol.* **200,** 46–56.

Morales, C. R., Oko, R., and Clermont, Y. (1994). Molecular cloning and developmental expression of an mRNA encoding the 27 kDa outer dense fiber protein of rat spermatozoa. *Mol. Reprod. Dev.* **37,** 229–240.

Mori, C., Nakamura, N., Welch, J. E., Gotoh, H., Goulding, E. H., Fujioka, M., and Eddy, E. M. (1998). Mouse spermatogenic cell-specific type 1 hexokinase (mHk1-s) transcripts are expressed by alternative splicing from the mHk1 gene and the HK1-S protein is localized mainly in the sperm tail. *Mol. Reprod. Dev.* **49,** 374–385.

Oko, R. (1988). Comparative analysis of proteins from the fibrous sheath and outer dense fibers of rat spermatozoa. *Biol. Reprod.* **39,** 169–182.

Oko, R. (1998). Occurrence and formation of cytoskeletal proteins in mammalian spermatozoa. *Andrologia* **30,** 193–206.

Oko, R., and Clermont, Y. (1988). Isolation, structure and protein composition of the perforatorium of rat spermatozoa. *Biol. Reprod.* **39,** 673–687.

Oko, R., and Clermont, Y. (1989). Light microscopic immunocytochemical study of fibrous sheath and outer dense fiber formation in the rat spermatid. *Anat. Rec.* **225,** 46–55.

Oko, R., and Maravei, D. (1994). Protein composition of the perinuclear theca of bull spermatozoa. *Biol. Reprod.* **50,** 1000–1014.

Olson, G. E., and Sammons, D. W. (1980). Structural chemistry of outer dense fibers of rat sperm flagellum. *Biol. Reprod.* **22,** 319–332.

Rivkin, E., Cullinan, E. B., Tres, L. L., and Kierszenbaum, A. L. (1997). A protein associated with the manchette during rat spermiogenesis is encoded by a gene of the TBP-1-like subfamily with highly conserved ATPase and protease domains. *Mol. Reprod. Dev.* **48,** 77–89.

Russell, L. D., Ying, L., and Overbeek, P. A. (1994). Insertional mutation that causes acrosomal hypo-development: Its relationship to sperm head shaping. *Anat. Rec.* **238,** 437–453.

Schafer, U. (1986). Genes for male specific transcripts in *Drosophila melanogaster. Mol. Gen. Genet.* **202,** 219–225.

Schafer, M., Borsch, D., Hulster, A., and Schafer, U. (1993). Expression of a gene duplication encoding conserved sperm tail proteins is translationally regulated in *Drosophila melanogaster. Mol. Cell. Biol.* **13,** 1708–1718.

Schalles, U., Shao, X., van der Hoorn, F. A., and Oko, R. (1998). Developmental expression of the 84-kDa ODF sperm protein: Localization to both the cortex and medulla of outer dense fibers and to the connecting piece. *Dev. Biol.* **199,** 250–260.

Schumacher, J. M., Lee, K., Edelhoff, S., and Braun, R. E. (1995). *Spnr,* a murine RNA-binding protein that is localized to cytoplasmic microtubules. *J. Cell Biol.* **129,** 1023–1032.

Schumacher, J. M., Artzt, K., and Braun, R. E. (1998). Spermatid perinuclear ribonucleic acid-binding protein binds microtubules *in vitro* and associates with abnormal manchettes *in vivo* in mice. *Biol. Reprod.* **59,** 69–76.

Shao, X., and van der Hoorn, F. A. (1996). Self-interaction of the major 27 kDa outer dense fiber protein is in part mediated by a leucine zipper domain. *Biol. Reprod.* **55,** 1343–1350.

Shao, X., Tarnasky, H. A., Schalles, U., Oko, R., and van der Hoorn, F. A. (1997). Leucine zippers mediate interactions of sperm tail-specific structural proteins. *J. Biol. Chem.* **272,** 6105–6113.

Tres, L. L., and Kierszenbaum, A. L. (1996). *Sak57,* an acidic keratin initially present in the spermatid manchette before becoming a component of paraaxonemal structures of the developing tail. *Mol. Reprod. Dev.* **44,** 395–407.

Tres, L. L., Rivkin, E., and Kierszenbaum, A. L. (1996). *Sak57,* an intermediate filament keratin present in intercellular bridges of rat primary spermatocytes. *Mol. Reprod. Dev.* **45,** 93–105.

Turner, K. J., Sharpe, R. M., Gaughan, J., Millar, M. R., Foster, P. M. D., and Saunders, P. T. K. (1997). Expression cloning of a rat testicular transcript abundant in germ cells, which contains two leucine zipper motifs. *Biol. Reprod.* **57,** 1223–1232.

Van der Hoorn, F. A., and Tarnasky, H. A. (1992). Factors involved in regulation of the RT7 promoter in a male germ cell-derived *in vitro* transcription system. *Proc. Natl. Acad. Sci. USA* **89,** 703–707.

Van der Hoorn, F. A., Tarnasky, H. A., and Nordeen, S. K. (1990). A new rat gene RT7 is specifically expressed during spermatogenesis. *Dev. Biol.* **142,** 147–154.

Vera, J. C., Brito, M., Zuvic, T., and Burzio, L. O. (1984). Polypeptide composition of rat sperm outer dense fibers. *J. Biol. Chem.* **259,** 5970–5977.

Vinson, C. R., Sigler, P. B., and McKnight, S. L. (1989). Scissors-grip model for DNA recognition by a family of leucine zipper proteins. *Science* **246,** 911–916.

Westhoff, D., and Kamp, G. (1997). Glyceraldehyde 3-phosphate dehydrogenase is bound to the fibrous sheath of mammalian spermatozoa. *J. Cell Sci.* **110,** 1821–1829.

Received for publication February 9, 1999
Revised April 7, 1999
Accepted April 7, 1999